Angewandte Chemie
GDCh
Eine Zeitschrift der Gesellschaft Deutscher Chemiker
www.angewandte.de

Akzeptierter Artikel

Titel: Pathways of Methane Transformation over Copper-Exchanged Mordenite as Revealed by in situ NMR and IR Spectroscopy

Autoren: Vitaly L. Sushkevich, René Verel, and Jeroen A. van Bokhoven

Dieser Beitrag wurde nach Begutachtung und Überarbeitung sofort als "akzeptierter Artikel" (Accepted Article; AA) publiziert und kann unter Angabe der unten stehenden Digitalobjekt-Identifizierungsnummer (DOI) zitiert werden. Die deutsche Übersetzung wird gemeinsam mit der endgültigen englischen Fassung erscheinen. Die endgültige englische Fassung (Version of Record) wird ehestmöglich nach dem Redigieren und einem Korrekturgang als Early-View-Beitrag erscheinen und kann sich naturgemäß von der AA-Fassung unterscheiden. Leser sollten daher die endgültige Fassung, sobald sie veröffentlicht ist, verwenden. Für die AA-Fassung trägt der Autor die alleinige Verantwortung.

Zitierweise: *Angew. Chem. Int. Ed.* 10.1002/anie.201912668
Angew. Chem. 10.1002/ange.201912668

Link zur VoR: http://dx.doi.org/10.1002/anie.201912668
http://dx.doi.org/10.1002/ange.201912668

WILEY-VCH

10.1002/ange.201912668

Pathways of Methane Transformation over Copper-Exchanged Mordenite as Revealed by *in situ* NMR and IR Spectroscopy

Vitaly L. Sushkevich[a,*], René Verel[b], Jeroen A. van Bokhoven[a,b,*]

[a] *Laboratory for Catalysis and Sustainable Chemistry, Paul Scherrer Institut, 5232 Villigen PSI, Switzerland*

[b] *Institute for Chemistry and Bioengineering, ETH Zurich, Vladimir-Prelog-Weg 1, 8093 Zurich, Switzerland*

Abstract

The reaction of methane with copper-exchanged mordenite with two different Si/Al ratios was studied by means of in situ NMR and infrared spectroscopies. The detection of NMR signals was shown to be possible with high sensitivity and resolution, despite the presence of a considerable number of paramagnetic Cu^{II} species. Several types of surface-bonded compounds were found after reaction, namely molecular methanol, methoxy species, dimethyl ether, mono- and bidentate formates, Cu^{I} monocarbonyl as well as carbon monoxide and dioxide, which were present in the gas phase. The relative fractions of these species are strongly influenced by the reaction temperature and the structure of the copper sites and are governed by the Si/Al ratio. While methoxy species bonded to Brønsted acid sites, dimethyl ether and bidentate formate species are the main products over copper-exchange mordenite with a Si/Al ratio of 6; molecular methanol and monodentate formate species were observed mainly over the material with a Si/Al ratio of 46. These observations are important for understanding the methane partial oxidation mechanism and for the rational design of the active materials for this reaction.

**Corresponding authors: Tel.: +41563103518; E-mail addresses: vitaly.sushkevich@psi.ch , jeroen.vanbokhoven@chem.ethz.ch.*

This article is protected by copyright. All rights reserved.

Accepted Manuscript

10.1002/ange.201912668

1. Introduction

The search for novel pathways for the conversion of methane to valuable chemicals nowadays attracts enormous interest from the industrial and scientific communities. [1-5] There is an abundance of natural gas, mostly methane, and its price is relatively low, when calculated per carbon fraction. However, methane is the least active of all the alkanes, and its selective transformation to the desired product is challenging. The common areas of research include methane dry reforming, [6, 7] non-oxidative aromatization [8, 9] and, more recently, direct oxidation to methanol [10-13]. The latter direction has attracted considerable attention in the last decade after it was discovered that copper-exchanged zeolites are able to activate methane. [14-17] To utilize this unique feature for practical applications, a chemical looping approach was suggested, implying cyclic exposure of the material, possessing redox properties, to an oxidant and to methane at different temperatures with the subsequent extraction of the oxidation products, typically by using water. [14-19] The activation of copper-containing materials is carried out at above 673K, while the reaction with methane and desorption of methanol requires lower temperatures to avoid over-oxidation. [10-13]

Numerous copper-exchanged zeolites, including CuMFI [14-18], CuMOR [19-26], CuFAU [27], CuMAZ [28-29] and CuCHA [30-34], were tested and revealed different methanol yields and selectivity per cycle. The research targeting the achievement of the highest methanol productivity allowed to obtain the methanol productivity close to the theoretical limit [35]. However, in most cases, it does not exceed ~100-150 μmol/g, thus accounting for ~0.2-0.3 mol(MeOH)/mol(Cu) [21-25, 28, 29, 33]. Equally, significant attention was given to the elucidation of the nature of copper-oxo active sites, hosted in different zeolites. Thus, PXRD, XAS, Raman and UV−vis data suggested that the formation of copper monomers [30, 36], dimers in a form of bis-μ-oxo [14, 15] and mono-μ-oxo [16, 17, 20] dicopper cores as well as trimers [21, 22] and copper oxide clusters [27, 32] is a possibility. The formation of these sites is governed by the topology of the zeolite [33, 35, 37], Si/Al ratio [18, 26, 33, 35], copper loading [29] and the nature of the counter-cation (H^+, Na^+ or NH_4^+) in the parent zeolite [22, 38]. During the reaction with methane, these sites undergo reduction, forming Cu^I species and methanol

This article is protected by copyright. All rights reserved.

Accepted Manuscript

with established stoichiometry of 2×Cu^{I} per one methanol molecule as calculated for 100% selectivity [29, 35, 39].

While copper transformation during activation in oxygen and reaction with methane has been the topic of considerable research, very little attention has been paid to the fate of reaction products originating from methane. Our first studies of this topic [23-25, 37] were based on in situ infrared spectroscopy, which revealed the formation of several types of methoxy and formate species and adsorbed carbon monoxide. Simultaneously, the formation of Brønsted acid sites was detected. [23] Furthermore, Oord et al. confirmed the formation of methoxy species by means of near-IR spectroscopy and detected ν(CH) overtones [40]. However, the nature, location and thermal stability of the surface species, which formed during the interaction of oxygen-activated copper-exchanged zeolites with methane, as well as the effect of the material composition and such characteristics as Si/Al ratio and copper loading, have not yet been studied in detail.

Here we present a systematic spectroscopic study of copper-exchanged mordenite with two different Si/Al ratios in the conversion of methane to methanol. Using in situ NMR and FTIR spectroscopy, we identified for the first time that multiple types of methoxy species, corresponding to molecular methanol, dimethyl ether (DME) and methoxy species bonded to Brønsted acid sites, form during the oxidation of methane. Reaction at relatively low temperature leads to the formation of a small amount of formaldehyde, while temperatures above 600 K lead to over-oxidation and formation of carbon monoxide and carbon dioxide, which readily desorb to the gas phase. Importantly, the samples with different Si/Al ratios, and, consequently, different structures of copper-oxo sites, react differently and show different fractions of molecular methanol and strongly bonded methoxy species. The study provides insight into methane oxidation over copper-exchanged zeolites at the molecular level and provides important information for the further improvement of the process and active material.

2. Results and discussion

Table 1 and Figs S1 to S6 give the characteristics of the samples used in the present study. Nitrogen adsorption-desorption data suggest a high micropore volume of the zeolites. CuMOR(6) and

This article is protected by copyright. All rights reserved.

Accepted Manuscript

CuMOR(46) reveal reversible Type-I adsorption/desorption isotherms with a step at $p/p_0 < 0.01$, typical of microporous solids (Fig. S1). The powder XRD patterns of all the samples show typical features of highly crystalline materials corresponding to a mordenite topology (Fig. S2). Reflections due to other phases of crystalline impurity phases were not detected, thus excluding the presence of large copper oxide particles. The nature of the Cu^{II} sites was also evaluated by infrared spectroscopy of adsorbed nitrogen monoxide, the comprehensive analysis of which was discussed elsewhere [24, 41]. It shows the preferential formation of copper-oxo monomeric species like $(CuOH)^+$ for CuMOR(46), while in the CuMOR(6) sample with a low Si/Al ratio, a mixture of copper sites with different nuclearity, including copper-oxo dimers [20] was found (for the details, please see Supporting Information Figs S3-S7). This is consistent with the low aluminum content of CuMOR(46), leading to the large statistical distance between two neighboring Al atoms in the zeolite framework, hence disabling the stabilization of copper oligomeric species. [42] Reactivity tests show the high activity of both CuMOR(6) and CuMOR(46) samples in the methanol synthesis, achieving 0.14 and 0.3 μmol(MeOH)/mol(Cu), respectively (Table 1). The selectivity measured at 473 K is above 90%, in line with previous studies [21, 23, 26]. Cycling the materials in five consecutive runs demonstrated stable methanol yield and selectivity, hence indicating the absence of significant deactivation under the selected conditions (Fig. S8).

First, the reaction of methane with CuMOR(6), activated in oxygen at 673 K to exclude the reduction with carbonaceous impurities [43], was studied at elevated temperature. ^{1}H MAS NMR spectra (Figs S9, S10) display the progressive development of the signal at 4.1 ppm due to the Brønsted acid sites, in line with our previous study, confirming that the reaction of Cu^{II} species in the zeolite pores with methane leads to the transfer of a hydrogen atom from CH_4 to the framework as a proton [23]. Simultaneously, the formation of Cu^{I} species is observed in Cu K edge XANES spectra acquired during the temperature-programmed reaction with methane (Fig. S11). These observations indicates the direct involvement of copper species to the reaction mechanism [26, 35, 39]. Fig. 1 shows ^{13}C HPDEC NMR spectra of reaction products as observed from 298 to 648 K. At ambient temperature, the only

This article is protected by copyright. All rights reserved.

Accepted Manuscript

signal was the broad signal at ~-6 ppm, corresponding to methane. [44-47] The strong broadening is associated with the presence of paramagnetic Cu^{II} species, which comprise most of the copper fraction in the activated copper-exchanged mordenite. An increase in the reaction temperature leads to narrowing of the methane signal due to the partial reduction of the paramagnetic Cu^{II} species to Cu^{I} with methane. Simultaneously, the signal position drifts from -6 to -10 ppm, which might be associated with different coordination and adsorption of methane over the surface of the material or different strength of paramagnetic pseudo-contact shift. The latter might arise from the interaction of methane with Cu^{II} sites leading to dipolar coupling between the magnetic moments of the ^{13}C nuclei and of the unpaired electron from Cu^{II}. [48] Starting at 448 K, a small signal appears at 58 ppm together with one at 67 ppm at slightly higher temperature (498 K), suggesting the formation of new carbon-containing species. The chemical shifts of these species are typical of compounds having C-O bonds and may correspond to CH_3O- fragments [49-55]. Further increase of the temperature leads to the development of signal at 124 due to carbon dioxide. [51, 52] Moreover, the careful analysis of the spinning side bands (Fig. S12) shows that another signal at 154 ppm having strong chemical shift anisotropy is present in the spectrum. The position of this band corresponds to carbon monoxide, which also can form stable Cu^{I} carbonyls, possessing the signals around 175 ppm in ^{13}C NMR spectrum. [53] Indeed, the latter can be observed in the spectra giving very weak and broad signals at 174 and 178 ppm, and can be only resolved by the analysis of spinning side bands appearing at 214, 218 and 253, 258 and 294, 298 ppm at 4 kHz MAS rate (for the details, please see Supporting Information, Fig. S12). Simultaneously, the intensities of the peaks at 58 and 67 ppm gradually decrease, indicating the over-oxidation of CH_3O- species to carbon oxides. The increase of the intensity of the peak due to carbon dioxide was not observed at high reaction temperatures. Most probably, this is associated with the adsorption of CO_2 over zeolite having non-reacted Cu^{II} species, which suppress ^{13}C signal (Fig. S13). None of other products, including alkenes or aromatics, were found in the spectra.

To access the structure and behavior of surface species, ^{1}H-^{13}C cross polarization spectra were collected (Fig. 2, Table S1). In contrast to ^{13}C HPDEC spectra, there were no signals due to methane,

This article is protected by copyright. All rights reserved.

Accepted Manuscript

carbon monoxide or carbon dioxide in the spectra. In the case of methane this suggests high mobility and weak bonding to the surface of copper-exchanged mordenite, implying preferential presence in the gas phase. The lack of carbon oxide signals in the CP/MAS spectra is associated with the absence of hydrogen atoms in the vicinity of carbon atoms, which restricts polarization transfer. Notably, the peaks within the range of 50 to 70 ppm persisted in the CP/MAS spectra, revealing the presence of at least five resolved signals at 52, 58, 62, 64 and 67 ppm. The high intensity in CP/MAS suggests the presence of multiple C-H bonds in these surface species, which, taken together with the chemical shift of the peaks, enables the assignment to CH_3O- fragments. Based on data reported previously and the discussion of the transformation of methanol over zeolitic materials lead to the attribution of the signal at 52 ppm to molecular methanol, which might bond weakly to the surface by H-bonding. [49-56] 2D ^{1}H-^{13}C heteronuclear correlation spectroscopy led to the assignment of the rest of the signals (Fig. 3). The major cross peaks appear at (58.5; 4.15), (64.1; 4.11), (67.2; 3.83) and (67.2; 3.13) ppm, confirming the attribution to the CH_3O- fragments. The first peak is typically observed over most of protonic forms of zeolites after adsorption and heating of methanol at elevated temperature and corresponds to the methoxy species bonded to the Brønsted acid sites [49, 50, 54]. The presence of multiple low-intensity cross-peaks at similar ^{13}C chemical shift, but ^{1}H chemical shift ranging from 4.8 to 5.8 ppm might be associated with the distortion of protons in methoxy species by the presence of other adsorbed molecules, formed during the oxidation of methane, in the pores of zeolite, the confinement effect of mordenite framework and presence of charged copper cations. Importantly, no resolved cross-peaks for ^{13}C signal at 62 ppm were observed in 2D ^{1}H-^{13}C HETCOR, making it difficult to attribute this signal with certainty. Literature data suggests that, during the transformation of methanol over copper-free mordenite at elevated temperature, there are no observable signals near 62 ppm in the ^{13}C NMR spectra [49, 50]. Equally, however, in copper-exchanged mordenite, the signal at 63 ppm was observed at 423 K, indicating the involvement of copper atoms in the coordination of these methoxy species. [51]

This article is protected by copyright. All rights reserved.

Accepted Manuscript

The signals at high frequencies are due to dimethyl ether formed from methanol via a dehydration reaction [21], with the signal at (64.1; 4.11) characteristic of dimethyl ether adsorbed over Brønsted acid sites, in side-on or end-on configuration. [51, 54] However, the presence of only one group of protons associated with this ^{13}C signal suggests the equality of both CH_3- groups in dimethyl ether and, hence, enables the attribution of the peak at 64.1 ppm to the end-on adsorbed DME. Interestingly, the ^{13}C peak at 67.2 ppm has two contributions from two different groups of protons at 3.13 and 3.83 ppm in ^{1}H NMR spectrum (Fig. 3). This clearly indicates the side-on coordination of dimethyl ether, which implies the presence of two unequal CH_3 groups. Furthermore, the shift to the high frequency suggests the coordination of DME to the strong electron-accepting site, which might be a Cu^{I} site, formed after the reduction of Cu^{II}-oxo species. We therefore attribute the ^{13}C signal to the side-on adsorbed DME at the ion-exchange position occupied by a Cu^{I} cation. The same attribution was proposed in the recent work by Zhou et al. [51]

With the exception of the formation of methoxy species and dimethyl ether, the heating of the sample to 498 to 548 K leads to the appearance of a new type of surface species with a ^{13}C signal at 173 ppm (Fig. 2). This is the spectroscopic signature of formate species, which can form from methoxy species or DME by further oxidation. Notably, this signal vanishes from the spectrum at 548 K, with simultaneous formation of carbon dioxide, as proven from the ^{13}C HPDEC NMR spectrum (Fig. 1). These observations suggest that the formate species are intermediates for carbon dioxide. The high temperature leads to a decrease in the intensity of the signals due to methoxy species and DME. Reaction at 598 K results in the disappearance of the signals at 64 and 67 ppm; further heating leads to a decrease in the intensity of the peaks at 52 and 58 ppm, thus indicating gradual thermal decomposition. Finally, at 648 K, there was only a small peak in the spectrum, due to the methoxy species bonded to the Brønsted acid sites. As such, dimethyl ether possesses low stability over the surface of copper-exchanged mordenite, and at temperatures as high as 598 K it undergoes oxidation to the mixture of carbon oxides. In contrast, the methoxy species and molecularly adsorbed methanol demonstrate high stability to over-oxidation at high temperature, probably due to the low mobility of

This article is protected by copyright. All rights reserved.

Accepted Manuscript

these species and hence disabling their diffusion to and reaction over the Cu^{II}-oxo active sites. Other products, such as aromatic or aliphatic compounds, were not observed at high temperature, which is consistent with previous studies reporting the exclusive formation of methanol and carbon oxides during methane oxidation over copper-exchanged mordenite. [14-35]

Due to the presence of a large amount of paramagnetic Cu^{II} in the activated sample, NMR spectroscopy is not sufficiently sensitive to the low concentration of reaction products, formed at low temperature when the conversion of Cu^{II} into Cu^{I} is low. In situ infrared spectroscopy was used to analyze the initial reaction products that form at the lowest temperature. The reaction conditions and experimental protocol for IR measurements were very similar to those used for the NMR measurements. Fig. 4 shows the IR spectra of surface species formed during the reaction of CuMOR(6) with methane at elevated temperature. Similar to the results of the NMR measurements, multiple bands, corresponding to different reaction products, are visible. Analysis of the intensity of the bands at increasing temperature enables assignment to five independent groups (Table 2, Fig. S14).

The bands belonging to the first and second groups appear in the spectra at the lowest temperatures and are due to the stretching and deformation vibrations in the CH_3O- fragments. These bands are present in the spectra staring from low temperature and develop progressively up to 598 K. Higher temperature leads to a decrease in the intensity; group (2) vanishes first. Comparing this behavior with NMR spectra (Fig. 2) suggests that group (1) corresponds to methoxy species bonded to the zeolite, while group (2) is associated with molecularly adsorbed methanol. This attribution is in line with literature data, showing a blue shift of the C-H stretching vibrations in methoxy species with respect to molecular methanol. [23, 57-59] The bands at 2159 cm^{-1} of group (3) are typical of carbon monoxide adsorbed over Cu^{I} and formed by thermal decomposition of formate, as revealed by NMR (Figs 1 and 2). The intensity of this band does not decrease, even at the highest temperature in these experiments, indicating the formation of highly stable $Cu^{I}(CO)$ monocarbonyl. [23, 60] Group (4), together with the various C-H vibrations, shows the presence of the bands at 1696 and 1685 cm^{-1}, which are characteristic of carbonyl compounds having a C=O group. Taking the chemistry of the

This article is protected by copyright. All rights reserved.

Accepted Manuscript

process into account, these bands may correspond to different forms of adsorbed formaldehyde, small amounts of which form from methanol or methoxy species during oxidation at low temperature. [61, 62] Formaldehyde is unstable at high temperature and decomposes rapidly, as visible in the IR spectra (Fig. 4). The last group (5) shows the superposition of several bands due to adsorbed water and asymmetric vibrations of formate species. [23, 63, 64] Both are formed by partial over-oxidation of methanol or methoxy species, formed from methane. The bands at 1619 and 1594 cm^{-1}, present between 448 and 548 K, are due to bidentate formate species. The increase in the reaction temperature above 548 K leads to the decomposition of formates and broadening of other signals, making the assignment challenging.

As well as the analysis of surface species, IR spectroscopy reveals the composition of the gas phase as a function of the reaction temperature. Fig. 5 presents the spectra collected upon heating of the CuMOR(6) sample in methane from 462 to 713 K. The bands at 2345 and 2144 cm^{-1} correspond to the stretching vibrations in carbon dioxide and carbon monoxide, respectively, while the broad band with fine structure, centered at 1300 cm^{-1}, is due to gaseous methane. The reaction at low temperature up to ~500 K does not lead to the formation of over-oxidation products: the absence of gaseous products suggests that the oxidation of formaldehyde observed in IR spectra (Fig. 4, Table S2) results in the formation of species adsorbed on the surface, presumably formate or adsorbed carbon monoxide. Progressive heating to 613 K leads to the appearance of the band due to carbon dioxide, the amount of which stabilizes and does not change at higher temperature (Fig. 5, Table S2). Compared with the behavior of surface formate species (Figs 2 and 4), the carbon dioxide that is released into the gas phase originates from the oxidation of surface formate species, which are unstable at high temperature over copper-exchanged mordenite. The formation of carbon dioxide from methoxy species or/and molecular methanol is less likely due to the stable amount of carbon dioxide in the gas phase, while the methoxy and methanol undergo progressive decomposition at temperatures above 600 K. Instead, at higher temperatures, the band due to gaseous carbon monoxide appears and develops gradually in the spectra (Fig. 5), which correlates with the decreasing intensity of the peaks due to methanol and methoxy

This article is protected by copyright. All rights reserved.

Accepted Manuscript

10.1002/ange.201912668

species in the NMR and IR spectra (Figs 2 and 4). Taken together, this suggests that over-oxidation of the latter at high temperature is complete and ceases at the stage of carbon monoxide formation.

Scheme 1 and Table 2 summarizes all these findings. The reaction of methane with activated copper-exchanged mordenite leads to the formation of molecular methanol and dimethyl ether, adsorbed on Brønsted acid sites, and methoxy species and carbon monoxide adsorbed over Cu^{I} sites. At low reaction temperature (≤473 K) formaldehyde may form, together with formate species, the latter being stable to ~550 K. Heating at higher temperatures results in the formation of carbon dioxide by oxidation of formate species and of carbon monoxide by oxidation of methoxy species, methanol and dimethyl ether.

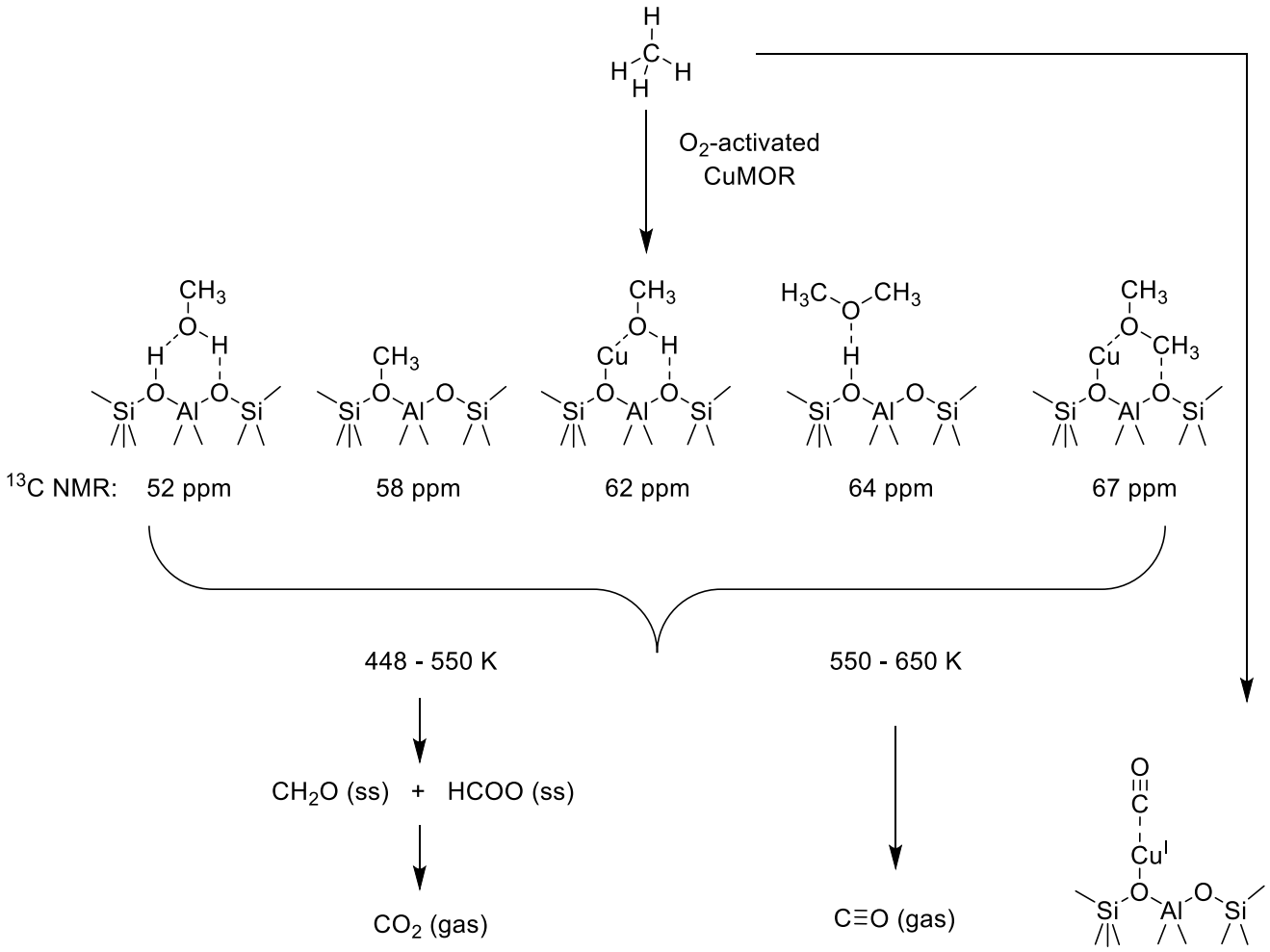

Scheme 1. Methane transformation pathways to the reaction products over CuMOR(6), revealed by NMR and IR spectroscopy.

This article is protected by copyright. All rights reserved.

Accepted Manuscript

Next we elucidated the effect of the structure of copper-oxo sites on the methane oxidation reaction. This required the study of the reaction over the CuMOR(46) sample, which predominantly contains the Cu^{II}-hydroxo monomeric species. It was recently shown that monomeric species are active in methane conversion and allows achieving higher selectivity with respect to that observed over the CuMOR(6) sample, which contains active sites with multiple copper atoms (see the Supporting Information). [24, 65] Similar results were reproduced for our CuMOR(46) material (Table 1). Fig. 6 shows the ^{13}C HPDEC NMR spectra of the reaction products formed after the reaction of activated CuMOR(46) with methane at elevated temperature. Compared to the spectra obtained for CuMOR(6), the intensity of the signal at -7 ppm due to gaseous methane is considerably higher, which is accounted for the smaller amount of paramagnetic copper loaded in the mordenite with a high Si/Al ratio. Reacting the sample at a temperature as high as 473 K leads to the appearance of a small signal at 52 ppm due to molecular methanol. In contrast to what is observed over CuMOR(6) (Fig. 1), heating at 648 K does not lead to a significant decrease in this signal or to the appearance of new signals as a result of over-oxidation. This indicates the high stability of the primary oxidation products over the CuMOR(46) sample, probably due to the isolated nature of the active Cu^{II}-hydroxo species.

^{13}C CPMAS NMR spectra of surface species acquired after reaction with methane (Fig. 7, S15) shows three signals at 52, 58 and 62 ppm, corresponding to molecular methanol and two types of methoxy species. Similar to CuMOR(6), the peak at 58 ppm is due to methoxy species bonded to Brønsted acid sites, while the assignment of the signal at 62 ppm remains speculative; the signal is probably associated with coordination of methoxy species to copper atoms. An increase in the reaction temperature leads to a gradual increase in the intensity of all the signals, indicating an increase in methane conversion and formation of molecular methanol rather than methoxy species in the studied temperature range. There are no other observable intense signals, including those due to dimethyl ether and formate species. The absence of DME as the reaction product might be associated with the low concentration of aluminum, which leads to the low concentration of Brønsted acid sites required for dehydration of methanol to dimethyl ether.

This article is protected by copyright. All rights reserved.

Accepted Manuscript

10.1002/ange.201912668

Fig. 8 shows in situ infrared spectra collected during the reaction of the CuMOR(46) sample with methane. Similar to that observed over CuMOR(6), the bands were associated with carbon monoxide adsorbed over Cu^{I} (2159 cm^{-1}) and adsorbed water (1628 cm^{-1}). In the C-H stretching range, there were no intense bands due to the methoxy species; the only intense bands at 2965($\nu_{as}(CH_3)$), 2959 ($\nu_{as}(CH_3)$) and 2858 cm^{-1} ($\nu_s(CH_3)$) correspond to molecular methanol. This is in line with ^{13}C NMR spectroscopy, revealing the presence of mostly molecular methanol adsorbed after reaction over CuMOR(46). Furthermore, a set of new bands, at 2921 (ν_{as}(HCO)), 2822 (ν_s(HCO)) and 1665 (ν_{as}(COO)) cm^{-1}, starting from ~500 K, developed. The positions of these bands are typical of formate species in monodentate coordination, which may form by over-oxidation of methanol and methoxy species. Formation of formate species, in contrast to what was found for CuMOR(6), was associated with the different nature of the copper-oxo sites in mordenite with a different Si/Al ratio. The intensity of all the bands in the IR spectra increased from 448 to 648 K, indicating the high stability of adsorbed methanol to over-oxidation as well as adsorbed carbon monoxide and formate species, which do not decompose and desorb into the gas phase, as was observed for the CuMOR(6) sample (Figs 4 and 5). No spectroscopic signatures of formaldehyde were detected in whole temperature range.

Scheme 2 summarizes the observations discussed above. Reaction of two isolated copper sites, represented by $CuOH^{+}$ species, leads to the formation of methoxy species, first coordinated to the reduced Cu^{I} motif and Brønsted acid sites with coordinated water. The formation of the latter is also confirmed by the FTIR spectroscopy, showing the appearance of the broad band at ~ 3400 cm^{-1} typical for the H-bonded water (Fig. S16). Then, methoxy species can undergo hydrolysis with coordinated water or other water molecules that form by over-oxidation of methane to form molecular methanol bonded to bridged hydroxyl groups of zeolite.

Accepted Manuscript

This article is protected by copyright. All rights reserved.

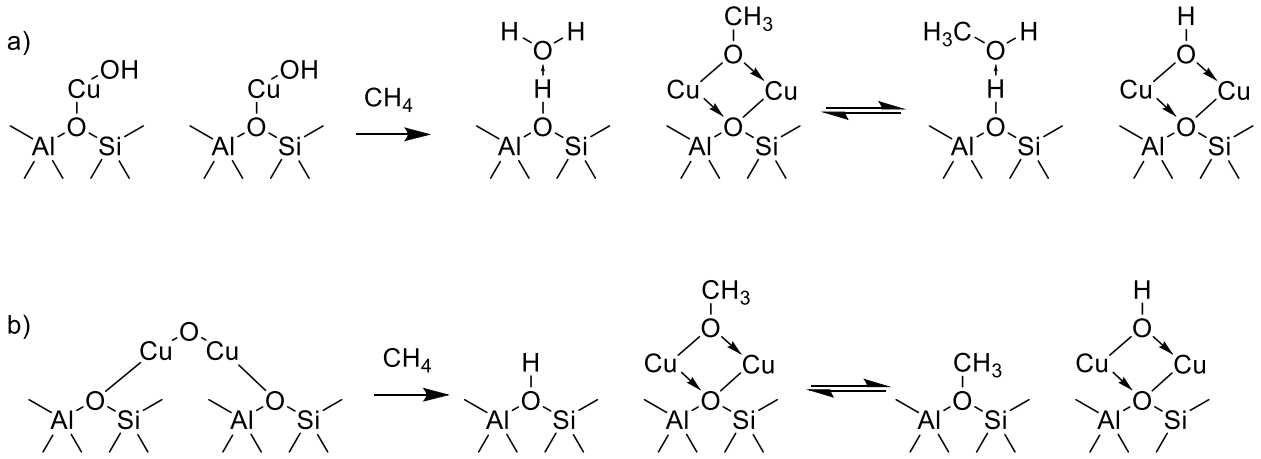

Scheme 2. Methane oxidation pathway over isolated copper-oxo species (a) and copper-oxo dimers (b), stabilized in mordenite with a high and low Si/Al ratio, respectively.

In the copper-exchanged mordenite sample with a low Si/Al ratio, in addition to the copper-oxo sites depicted in Scheme 2, the formation of copper-oxo oligomers, such as dicopper mono-μ-oxo species, is possible [20, 26, 35]. The pathway, describing the reaction of such sites with methane is given in Scheme 2b. Due to the absence of hydrogen atoms in mono-μ-oxo species, the reaction with methane results in the formation of free Brønsted acid sites together with a reduced Cu^{I} motif (Scheme 2). Methoxy species can migrate to these Brønsted acid sites and form stable species, as observed by NMR and IR spectroscopy.

The above schemes explain the dominant formation of molecular methanol over CuMOR(46) with respect to CuMOR(6), where methoxy species are the main product. The reduction of two $CuOH^{+}$ sites leads to the formation of one water molecule per one methoxy fragment. This water reacts with methoxy species to give molecular methanol. In the case of the reaction of methane with mono-μ-oxo species, no additional water is formed, hence stabilizing the methoxy species on Brønsted acid sites. The only that is water formed by over-oxidation at high temperature and promotes hydrolysis, leading to molecular methanol, a small amount of which is visible in the spectra starting from 548 K for CuMOR(6) (Figs 2 and 4).

Further transformation of methoxy species and methanol implies the conversion to dimethyl ether and over-oxidation to the formate species, CO and CO_2. The formation of DME is pronounced over the sample with a low Si/Al ratio, i.e. a high aluminum content, which forms Brønsted acid sites

This article is protected by copyright. All rights reserved.

Accepted Manuscript

that catalyze the dehydration reaction of methanol. The sample with a high Si/Al ratio is more selective to methanol, showing no significant signals due to carbon oxides in the NMR spectra (Figs 1 and 6). The nature of formate species over copper-exchanged mordenites depends on the Si/Al ratio: For CuMOR(6) mostly bidentate formate forms, while the reaction of CuMOR(46) with methane leads to monodentate formate species. The reasons for this are presumably associated with the different structure of the copper active sites in the studied materials.

3. Conclusions

Depending on the temperature, the reaction of methane with oxygen-activated copper-exchanged mordenite leads to the formation of multiple surface species and gas phase products. The Si/Al ratio of zeolite affects the structure of the copper species and is mainly responsible for the formation of different products. At a temperature between 448 and 573 K the formation of molecular methanol, methoxy species bonded to Brønsted acid sites and copper sites, as well as dimethyl ether and formate species was detected. Dimethyl ether forms by dehydration of the methanol pathway, while formate species are the unstable products of over-oxidation, which undergo thermal decomposition to carbon dioxide. The reaction at higher temperatures from 573 to 648 K results in severe over-oxidation of methoxy species, dimethyl ether and methanol to carbon monoxide.

The structure of the copper active sites, which can be modulated by changing the Si/Al ratio of the parent zeolite, has a significant effect on the relative fraction and the nature of the reaction products. Specifically, the reaction of CuMOR with s high Si/Al ratio, stabilizing the formation of isolated copper-hydroxo sites in the zeolite pores, with methane, leads to the formation of mainly molecular methanol. In contrast, over CuMOR with a low Si/Al ratio, methoxy species dominate. This is associated with the contribution of the copper-oxo oligomers, such as dicopper mono-μ-oxo sites, which react with methane, and does not lead to the formation of water, capable of methoxy hydrolysis.

Finally, NMR spectroscopy can be applied successfully to the study of oxygen-activated copper-exchange zeolites, in spite of the presence of a large amount of paramagnetic Cu^{II} species. This opens up new possibilities for studying the reaction mechanisms over this important class of materials.

This article is protected by copyright. All rights reserved.

Accepted Manuscript

4. Supporting information

Nitrogen adsorption-desorption isotherms, XRD patterns, FTIR spectra of adsorbed nitrogen monoxide and carbon dioxide, temperature-programmed reaction with methane followed by Cu K edge XANES, ^{1}H MAS NMR spectra, ^{1}H-^{13}C HETCOR of CuMOR(46), spinning side bands analysis, full-range FTIR spectra after reaction with methane, table with NMR signals assignment.

5. Acknowledgements

V.L.S. and J.A.v.B thank the Energy System Integration platform of the Paul Scherrer Institute for financial support.

6. References

(1) J.-P. Lange, K. P. de Jong, J. Ansorge, P. J. Tijm, Stud. Surf. Sci. Catal., 1997, 107, 81-86.

(2) R. Periana, D. Taube, S. Gamble, H. Taube, T. Satoh, H. Fujii, Science, 1998, 280, 560-564.

(3) A. I. Olivos-Suarez, À. Szécsényi, E. J. M. Hensen, J. Ruiz-Martinez, E. A. Pidko, J. Gascon, ACS Catal., 2016, 6, 2965–2981.

(4) P. Tomkins, M. Ranocchiari and J. A. van Bokhoven, Acc. Chem. Res., 2017, 50, 418–425.

(5) A. R. Kulkarni, Z.-J. Zhao, S. Siahrostami, J. K. Nørskov, F. Studt, Catal. Sci. Technol., 2018, 8, 114-123.

(6) Mette, K.; Kühl, S.; Tarasov, A.; Willinger, M. G.; Kröhnert, J.; Wrabetz, S.; Trunschke, A.; Scherzer, M.; Girgsdies, F.; Düdder, H.; Kähler, K.; Ortega, K. F.; Muhler, M.; Schlögl, R.; Behrens, M.; Lunkenbein, T., ACS Catal. 2016, 6, 7238-7248.

(7) Verykios, X., Appl. Catal. A 2003, 255, 101-111.

(8) J. Spivey, G. Hutchings, Chem. Soc. Rev., 2014, 43, 792-803.

(9) N. Kosinov, F. Coumans, G. Li, E. Uslamin, B. Mezari, A.Wijpkema, E. Pidko, E. Hensen, J. Catal., 2017, 346, 125-133.

(10) M. Ahlquist, R. J. Nielsen, R. A. Periana, W. A. Goddard, J. Am. Chem. Soc., 2009, 131, 17110-17115.

This article is protected by copyright. All rights reserved.

Accepted Manuscript

(11) J. T. Fuller, S. Butler, D. Devarajan, A. Jacobs, B. Hashiguchi, M. Konnick, W. Goddard, J. Gonzales, R. Periana, D. Ess, ACS Catal., 2016, 6, 4312-4322.

(12) M. Ravi, M. Ranocchiari, J. A. van Bokhoven, Angew. Chem., Int. Ed., 2017, 56, 16464-16483.

(13) A. Latimer, A. Kulkarni, H. Aljama, J. Montoya, J. S. Yoo, C. Tsai, F. Abild-Pedersen, F. Studt, J. Nørskov, Nat. Mat., 2017, 16, 225-229.

(14) M. H. Groothaert, P. J. Smeets, B. F. Sels, P. A. Jacobs, R. A. Schoonheydt, J. Am. Chem. Soc., 2005, 127, 1394–1395.

(15) P.J. Smeets, M.H. Groothaert, R.A. Schoonheydt, Catal. Today, 2005, 110, 303-309.

(16) J. S. Woertink, P. J. Smeets, M. H. Groothaert, M. A. Vance, B. F. Sels, R. A. Schoonheydt, E. I. Solomon, Proc. Natl. Acad. Sci. U. S. A., 2009, 106, 18908–18913.

(17) P. J. Smeets, R. G. Hadt, J. S. Woertink, P. Vanelderen, R. A. Schoonheydt, B. F. Sels, E. I. Solomon, J. Am. Chem. Soc., 2010, 132, 14736–14738.

(18) P. Vanelderen, R. G. Hadt, P. J. Smeets, E. I. Solomon, R. A. Schoonheydt, B. F. Sels, J. Catal., 2011, 284, 157–164.

(19) E. M. Alayon, M. Nachtegaal, M. Ranocchiari, J. A. van Bokhoven, Chem. Commun., 2012, 48, 404–406.

(20) P. Vanelderen, B. E. R. Snyder, M.-L. Tsai, R. G. Hadt, J. Vancauwenbergh, O. Coussens, R. A. Schoonheydt, B. F. Sels, E. I. Solomon, J. Am. Chem. Soc., 2015, 137, 6383–6392.

(21) S. Grundner, M. A. C. Markovits, G. Li, M. Tromp, E. A. Pidko, E. J. M. Hensen, A. Jentys, M. Sanchez-Sanchez, J. A. Lercher, Nat. Commun., 2015, 6, ncomms8546.

(22) S. Grundner, W. Luo, M. Sanchez-Sanchez, J. A. Lercher, Chem. Commun., 2016, 52, 2553–2556.

(23) V. L. Sushkevich, D. Palagin, M. Ranocchiari, J. A. van Bokhoven, Science, 2017, 356, 523-527.

This article is protected by copyright. All rights reserved.

Accepted Manuscript

(24) V.L. Sushkevich, D. Palagin, J.A. van Bokhoven, Angew. Chem. Int. Ed., 2018, 57, 8906-8910.

(25) V.L. Sushkevich, J.A. van Bokhoven, Catal. Sci. Technol., 2018, 8, 4141-4150.

(26) K. Lomachenko, A. Martini, D. Pappas, C. Negri, M. Dyballa, G. Berlier, S. Bordiga, C. Lamberti, U. Olsbye, S. Svelle, P. Beato, E. Borfecchia, Catal . Today, 2019, DOI: 10.1016/j.cattod.2019.01.040

(27) P. Tomkins, A. Mansouri, S. E. Bozbag, F. Krumeich, M. B. Park, E. M. C. Alayon, M. Ranocchiari, J. A. van Bokhoven, Angew. Chem. Int. Ed., 2016, 128, 5557–5561.

(28) M. B. Park, S. H. Ahn, A. Mansouri, M. Ranocchiari, J. A. van Bokhoven, ChemCatChem, 2017, 9, 3705-3713.

(29) A. J. Knorpp, A. Pinar, M. Newton, V. Sushkevich, J. van Bokhoven, ChemCatChem, 2018, 10, 5593-5596.

(30) M. J. Wulfers, S. Teketel, B. Ipek, R. F. Lobo, Chem. Commun., 2015, 51, 4447–4450.

(31) B. Ipek, R. F. Lobo, Chem. Commun., 2016, 52, 13401–13404.

(32) B. Ipek, M. Wulfers, H. Kim, F. Göltl, I. Hermans, J. Smith, K. Booksh, C. Brown, R. Lobo, ACS Catal., 2017, 7, 4291-4303.

(33) D. K. Pappas, E. Borfecchia, M. Dyballa, I. Pankin, K. A. Lomachenko, A. Martini,M. Signorile, S. Teketel, B. Arstad, G. Berlier, J. Am. Chem. Soc., 2017, 139, 14961-14975.

(34) E. Borfecchia, D. Pappas, M. Dyballa, K. Lomachenko, C. Negri, M. Signorile, G. Berlier, Catal. Today, 2019, 333, 17-27.

(35) D. Pappas, A. Martini, M. Dyballa, K. Kvande, S. Teketel, K. Lomachenko, R. Baran, P. Glatzel, B. Arstad, G. Berlier, C. Lamberti, S. Bordiga, U. Olsbye, S. Svelle, P. Beato, E. Borfecchia, J. Am. Chem. Soc., 2018, 140, 15270-15278.

(36) A. R. Kulkarni, Z.-J. Zhao, S. Siahrostami, J. K. Nørskov, F. Studt, ACS Catal., 2016, 6, 6531–6536.

(37) V. L. Sushkevich, J.A. van Bokhoven, ACS Catal., 2019, 9, 6293-6304.

This article is protected by copyright. All rights reserved.

Accepted Manuscript

(38) K. Narsimhan, K. Iyoki, K. Dinh, Y Román-Leshkov, ACS Cent. Sci., 2016, 2, 424-429.

(39) M. Newton, A. Knorpp, A. Pinar, V. Sushkevich, D. Palagin, J. van Bokhoven, J. Am. Chem. Soc., 2018, 140, 10090-10093.

(40) R. Oord, J. Schmidt, B. M. Weckhuysen, Catal. Sci. Technol., 2018, 8, 1028-1038.

(41) V. L. Sushkevich, A.V. Smirnov, J.A. van Bokhoven, J. Phys. Chem. C., 2019, 123, 9926-9934.

(42) S. Brandenberger, O. Kröcher, A. Tissler and R. Althoff, Appl. Catal., A, 2010, 373, 168–175.

(43) V.L. Sushekvich, J.A. van Bokhoven, Chem. Commun., 2018, 54, 7447-7450.

(44) R. Harris, E. Becker, S. Cabral de Menezes, R. Goodfellow, P. Granger, Concepts in Magnetic Resonance, 2002, 14, 326 –346.

(45) A.G. Stepanov, Zeolites and Zeolite-like Materials, Elsevier, 2016.

(46) A. A. Gabrienko, S. S. Arzumanov, I. B. Moroz, A. V. Toktarev, W. Wang, A. G. Stepanov, J. Phys, Chem, C., 2013, 117, 7690-7702.

(47) M. V. Luzgin,V. A. Rogov, S. S. Arzumanov, A. V. Toktarev, A. G. Stepanov, V. N. Parmon, Angew. Chem. Int. Ed., 2008, 47, 4559-4562.

(48) H. M. McConnell, R. E. Robertson, J. Chem. Phys., 1958, 29, 1361-1365.

(49) Y. Jiang, M. Hunger, W. Wang, J. Am. Chem. Soc., 2006, 128, 11679-11692.

(50) T. Blasco, M. Boronat, P. Concepción, A. Corma, D. Law, J. A. Vidal-Moya, Angew. Chem. Int. Ed., 2007, 46, 3938-3941.

(51) L. Zhou, S. Li, G. Qi, Y. Su, J. Li, A. Zheng, X. Yi, Q. Wang, F. Deng, Solid State Nucl. Magn., Res., 2016, 80, 1-6

(52) B. Li, J. Xu, B. Han, X. Wang, G. Qi, Z. Zhang, C. Wang, F. Deng, J. Phys. Chem. C, 2013, 117, 5840-5847

(53) M. Hartmann, B. Boddenberg, Stud. Surf. Sci. Catal., 1994, 84, 509-517.

(54) W. Wang, M. Hunger, Acc. Chem. Res., 2008, 41, 895-904.

This article is protected by copyright. All rights reserved.

Accepted Manuscript

(55) E. V. Starokon, M. V. Parfenov, S. S. Arzumanov, L. V. Pirutko, A. G. Stepanov, G. I. Panov, J. Catal., 2013, 300, 47-54.

(56) M. V. Luzgin, M. S. Kazantsev, W. Wang, A. G. Stepanov, J. Phys. Chem. C., 2009, 113, 19639-19644.

(57) Y. Zhang, D. N. Briggs, E. Smit, A. T. Bell, J. Catal., 2007, 251, 443-452.

(58) S. M. Campbell, X.-Z. Jiang, R. F. Howe, Micropor. Mesopor. Mater., 1999, 29, 91-108.

(59) A. J. Jones, E. Iglesia, Angew. Chem. Int. Ed., 2014, 53, 12177-12181.

(60) G. Turnes Palomino, S. Bordiga, A. Zecchina, G. L. Marra, C. Lamberti, J. Phys. Chem. B., 2000, 104, 8641-8651.

(61) E. Kukulska-Zając, J. Datka, J. Phys. Chem. C., 2007, 111, 3471-3475.

(62) F.X. Llabrés i Xamena, C. Otero Areán, S. Spera, E. Merlo, A. Zecchina, Catal. Lett., 2004, 95, 51-55.

(63) K. K. Bando, K. Sayama, H. Kusama, K. Okabe, H Arakawa, Appl. Cata. A: Gen., 1997, 165, 391-409.

(64) M. Marwood, R. Doepper, A. Renken, "Appl. Cata. A: Gen., 1997, 151, 223-246.

(65) J. Meyet, K. Searles, M. Newton, M. Wörle, A. van Bavel, A. D. Horton, J. A. van Bokhoven, C. Copéret, Angew. Chem. Int. Ed., 2019, 58, 9841-9845.

Accepted Manuscript

This article is protected by copyright. All rights reserved.

10.1002/ange.201912668

Table 1. Characteristics of studied copper-exchanged mordenites

Sample	Elemental composition		V_{micro}, cm^3/g	Methanol yield, mol_{MeOH}/mol_{Cu}	Selectivity towards methanol, %
	Si/Al ratio	Cu loading, wt%			
CuMOR(6)	6.5	4.36	0.19	0.14	92
CuMOR(46)	46.1	1.22	0.18	0.30	98

Table 2. Assignment of IR bands observed during the reaction of copper-exchanged mordenites with methane at elevated temperature. Mind that the deconvolution of the bands at 1458 and 1469 cm^{-1} due to the deformation vibrations of CH_3 group in methanol and methoxy species is complicated to and the therefore the assignment was based on the literature data.

Group	Assignment	IR band frequencies, cm^{-1}
1	Methoxy species bonded to Brønsted acid sites	2980 ($\nu_{as}(CH_3)$), 2871 ($\nu_s(CH_3)$), 1458 ($\delta(CH_3)$)
2	Molecularly adsorbed methanol	2967 ($\nu_{as}(CH_3)$), 2856 ($\nu_s(CH_3)$), 1469 ($\delta(CH_3)$)
3	Cu^I monocarbonyl	2159 ($\nu(CO)$)
4	Adsorbed formaldehyde	2942 ($\nu_{as}(CH_3)$), 2836 ($\nu_s(CH_3)$), 1696 ($\nu(C=O)$), 1685 ($\nu(C=O)$), 1491 ($\delta(CH_3)$)
5	Overlapping bands from adsorbed water and formate species	1632 ($\delta(H_2O)$), 1619 ($\nu_{as}(COO)$), 1594 ($\nu_{as}(COO)$)

Accepted Manuscript

This article is protected by copyright. All rights reserved.

10.1002/ange.201912668

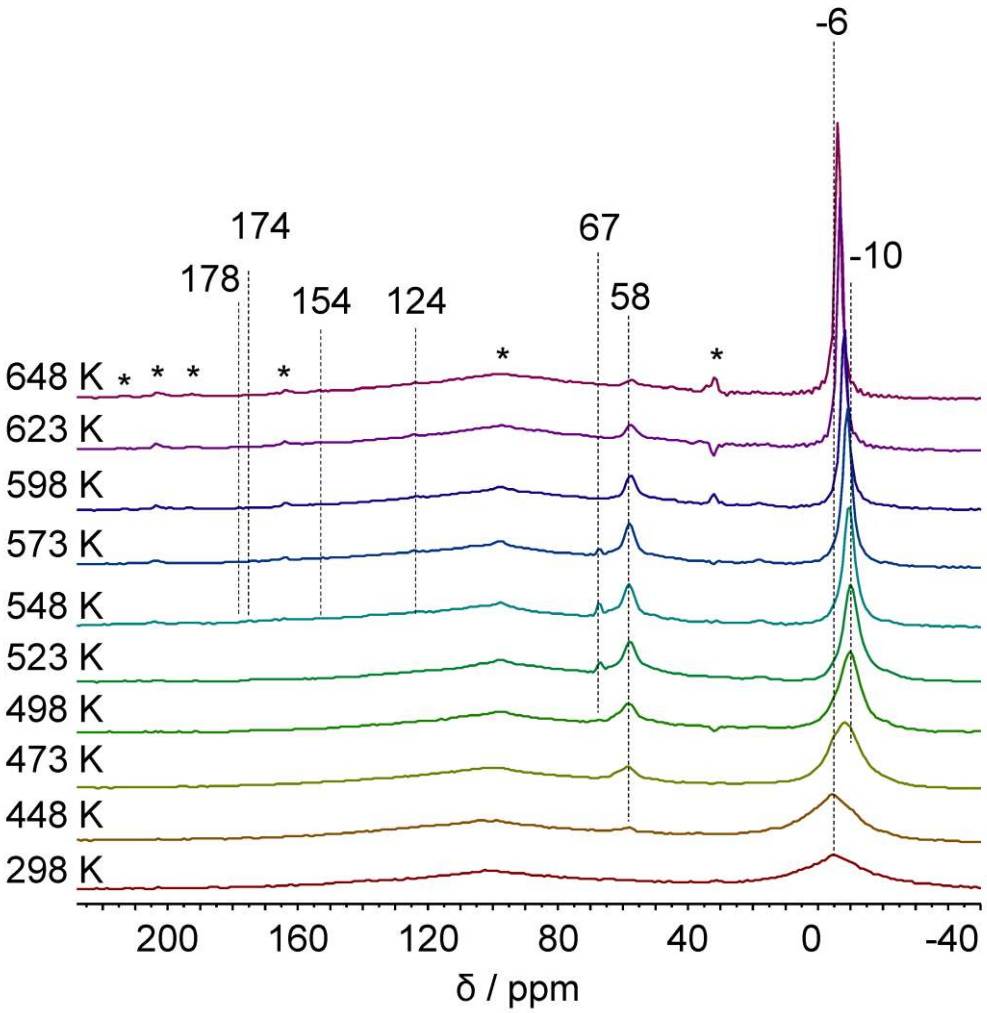

Fig. 1. ^{13}C HPDEC MAS NMR spectra of CuMOR(6) after the reaction with methane for 5 min at the temperatures from 298 to 648K. Asterisks denote the broad contribution from NMR probe and spinning side bands.

Accepted Manuscript

This article is protected by copyright. All rights reserved.

10.1002/ange.201912668

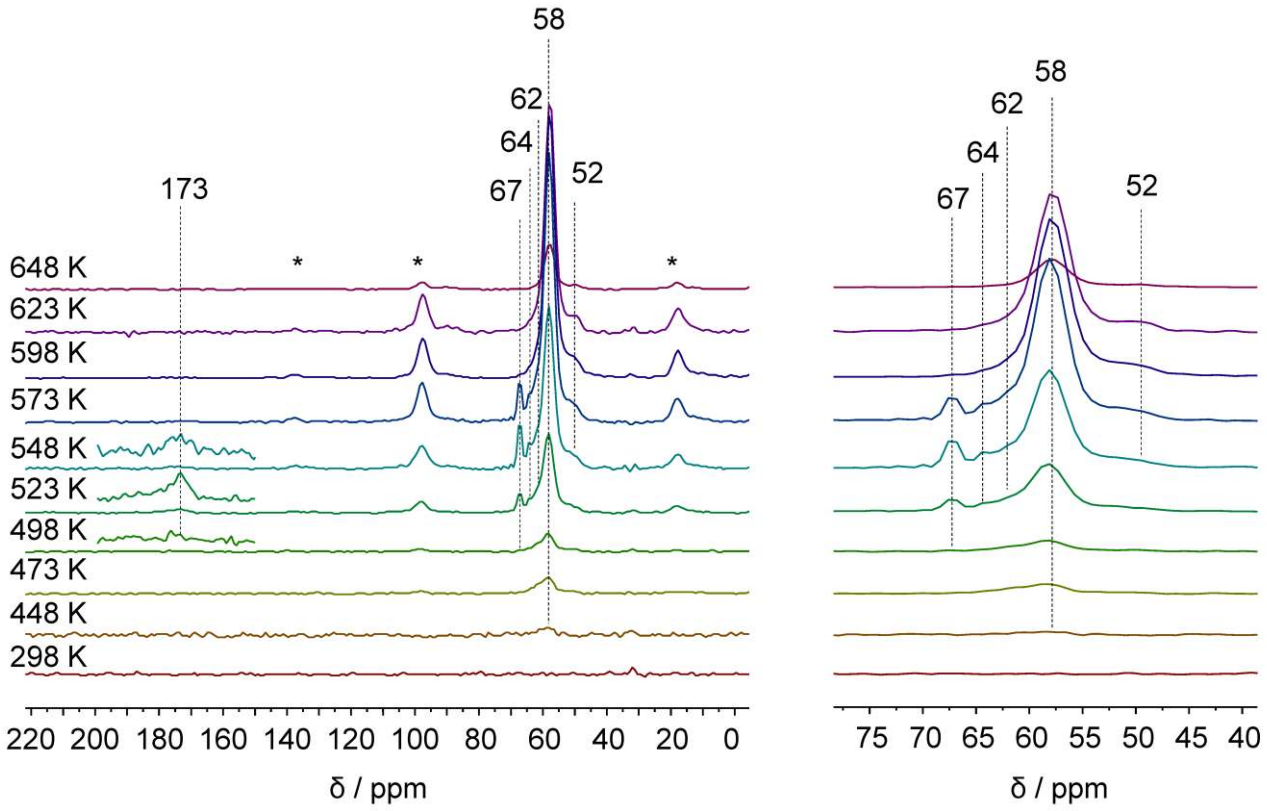

Fig. 2. ^{13}C CP/MAS NMR spectra of CuMOR(6) after the reaction with methane for 5 min at the temperatures from 298 to 648K. Asterisks denote the spinning side bands.

Accepted Manuscript

This article is protected by copyright. All rights reserved.

10.1002/ange.201912668

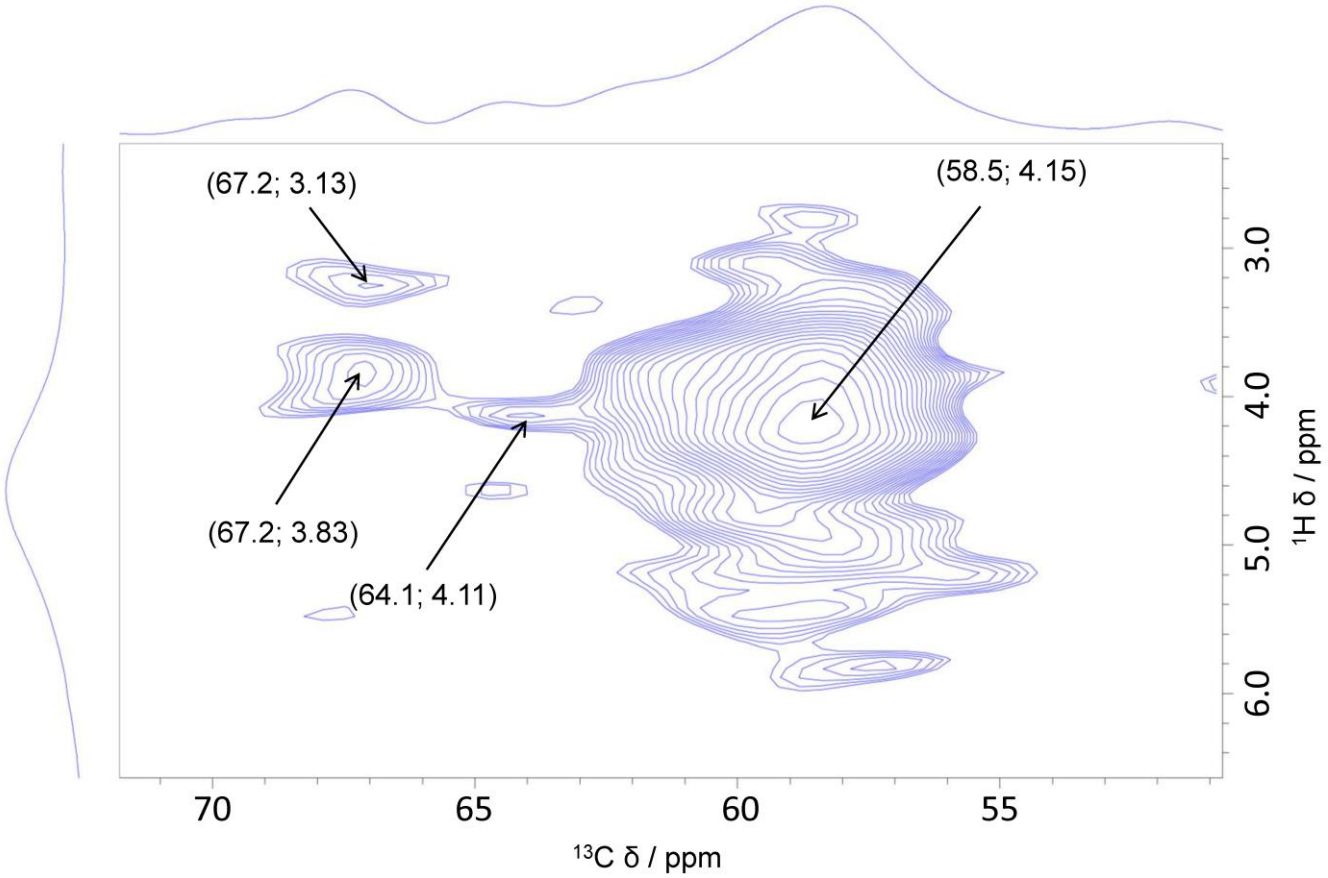

Fig. 3. ^{1}H-^{13}C HETCOR MAS NMR spectra of CuMOR(6) after the reaction with methane for 5 min at 523K.

Accepted Manuscript

This article is protected by copyright. All rights reserved.

10.1002/ange.201912668

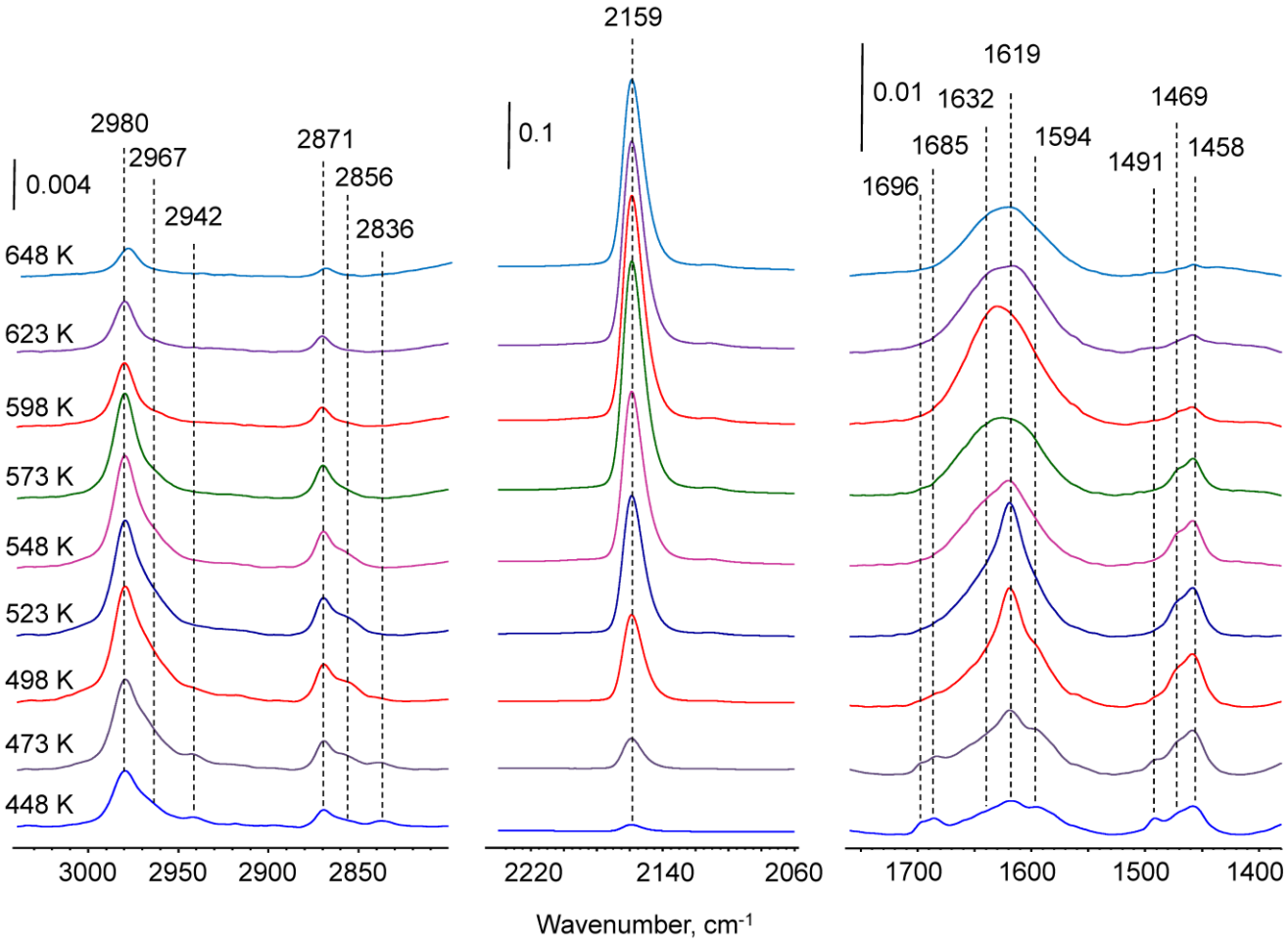

Fig. 4. IR spectra of surface species formed after the reaction of CuMOR(6) with 200 torr of methane for 5 min at the temperatures from 298 to 648K.

Accepted Manuscript

This article is protected by copyright. All rights reserved.

10.1002/ange.201912668

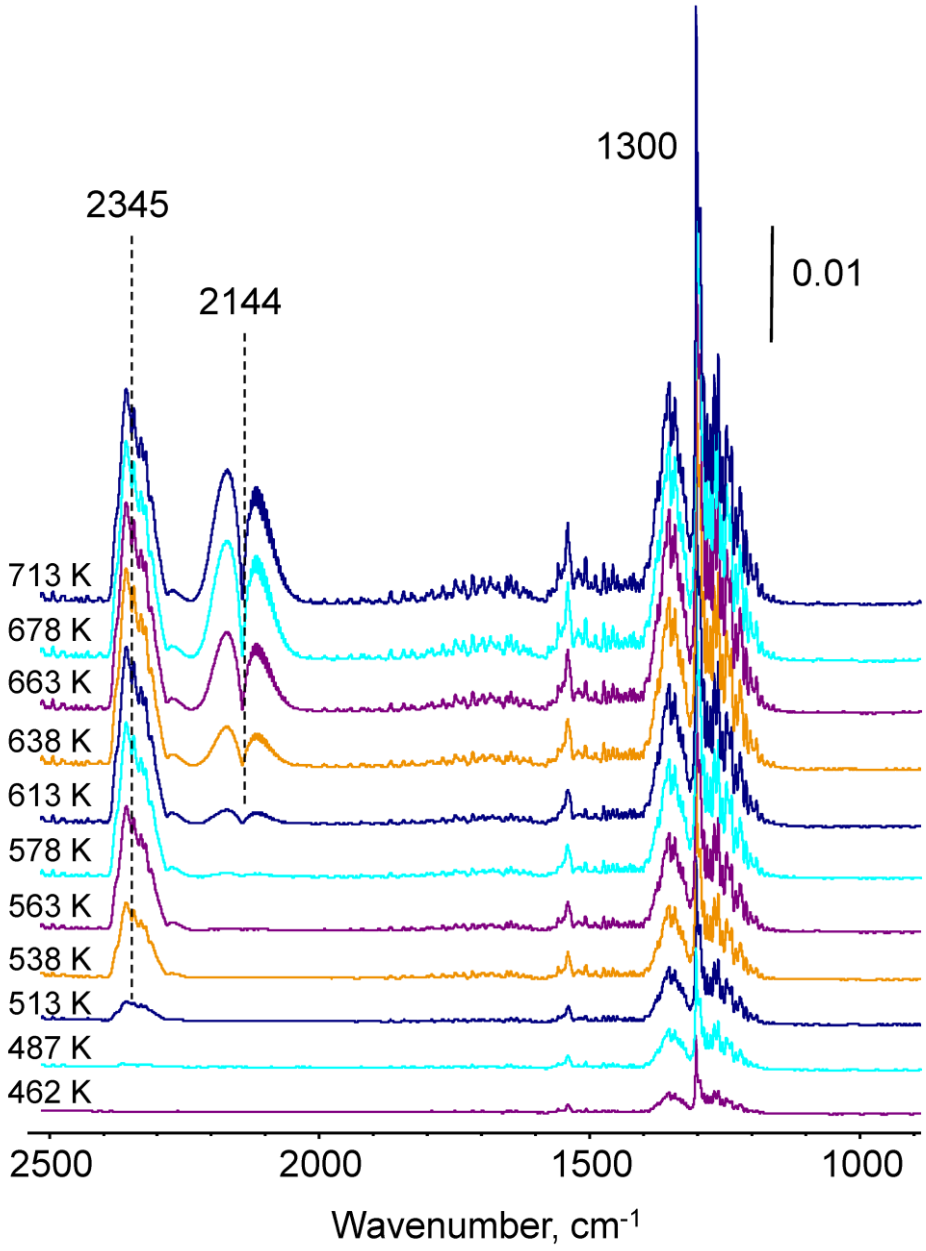

Fig. 5. IR spectra of gas phase acquired during the reaction of CuMOR(6) with 200 torr of methane at elevated temperature.

Accepted Manuscript

This article is protected by copyright. All rights reserved.

10.1002/ange.201912668

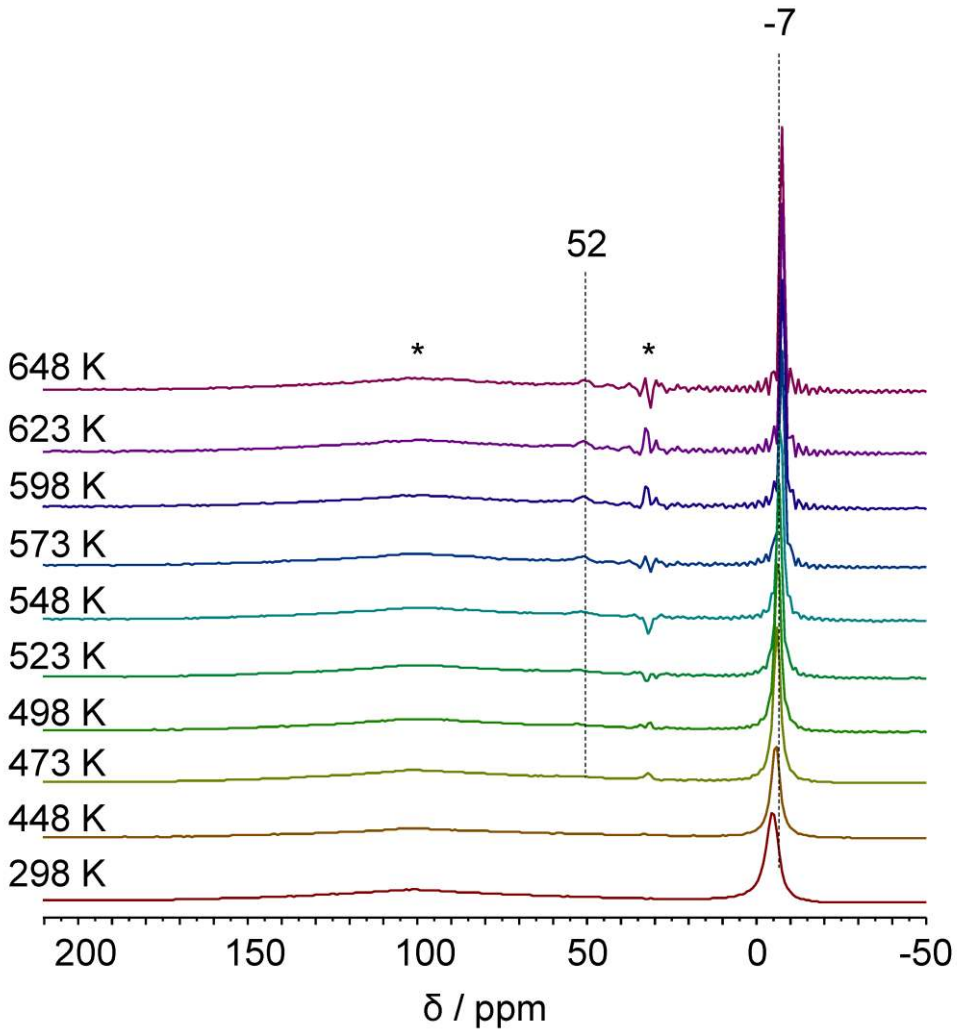

Fig. 6. ^{13}C HPDEC MAS NMR spectra of CuMOR(46) after the reaction with methane for 5 min at the temperatures from 298 to 648K. Asterisks denote the broad contribution from NMR probe and spinning side bands, the wiggles around the signal at -7 ppm arise from the use of short acquisition times.

Accepted Manuscript

This article is protected by copyright. All rights reserved.

10.1002/ange.201912668

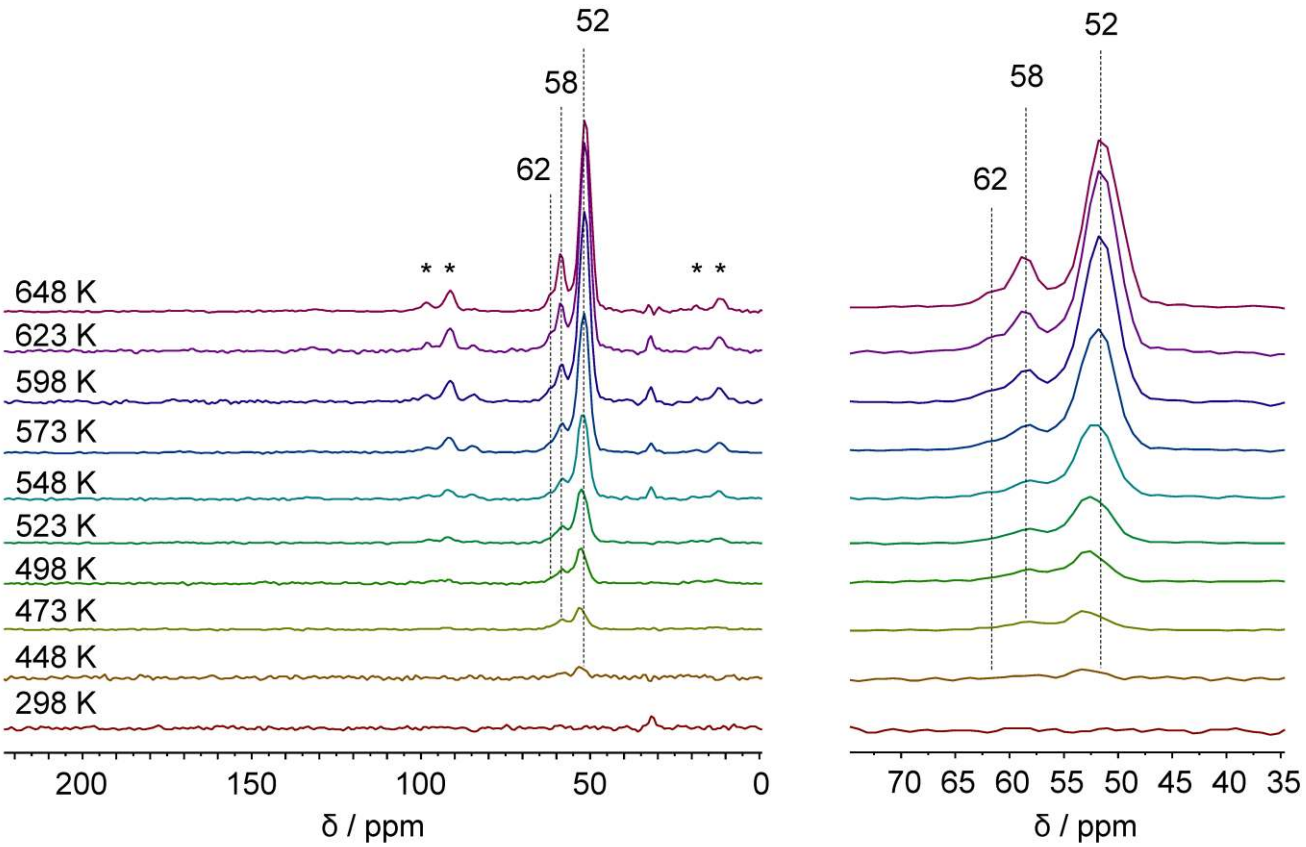

Fig. 7. ^{13}C CP/MAS NMR spectra of CuMOR(46) after the reaction with methane for 5 min at the temperatures from 298 to 648K. Asterisks denote the spinning side bands.

Accepted Manuscript

This article is protected by copyright. All rights reserved.

10.1002/ange.201912668

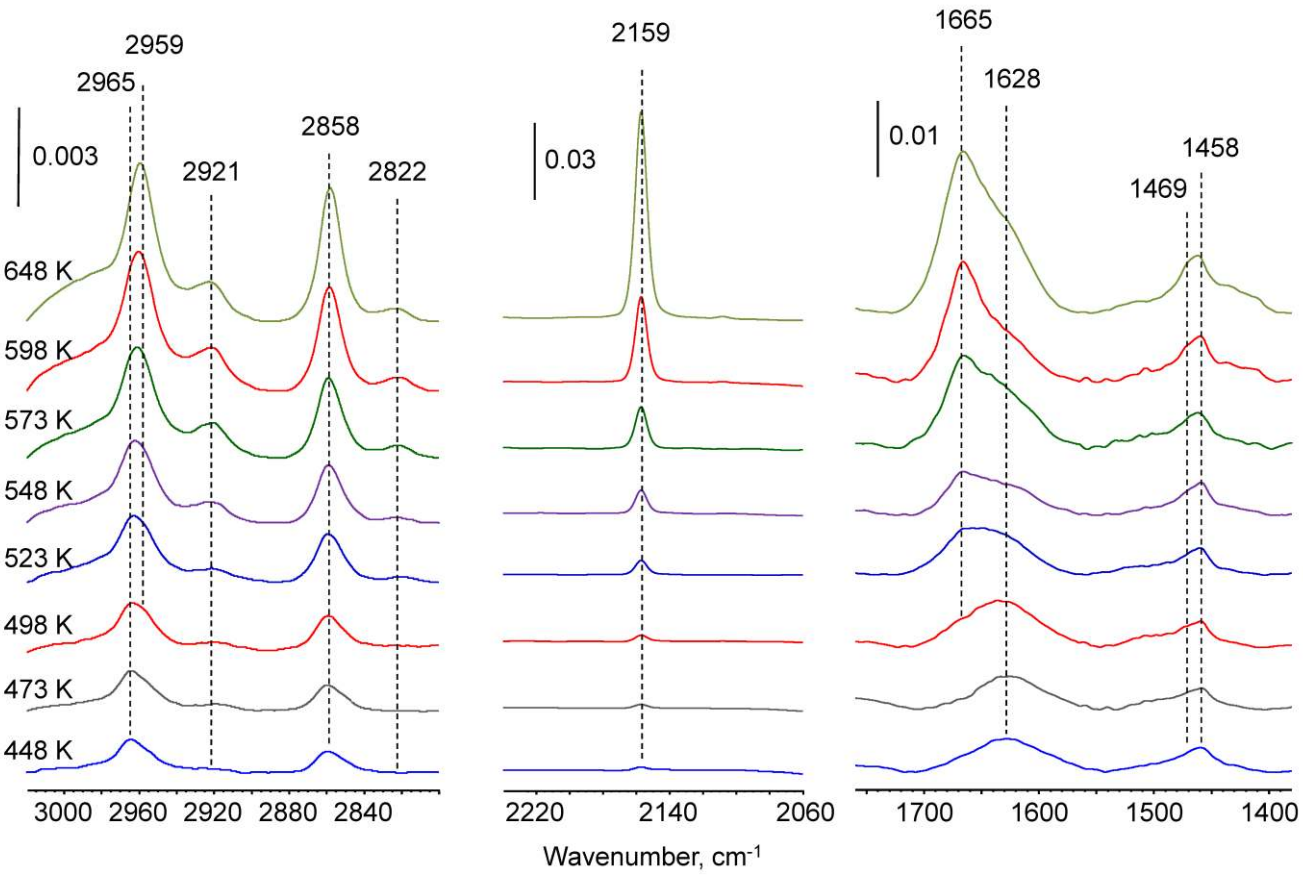

Fig. 8. IR spectra of surface species formed after the reaction of CuMOR(46) with 200 torr of methane for 5 min at the temperatures from 298 to 648K.

Accepted Manuscript

This article is protected by copyright. All rights reserved.

10.1002/ange.201912668

TOC Graphic

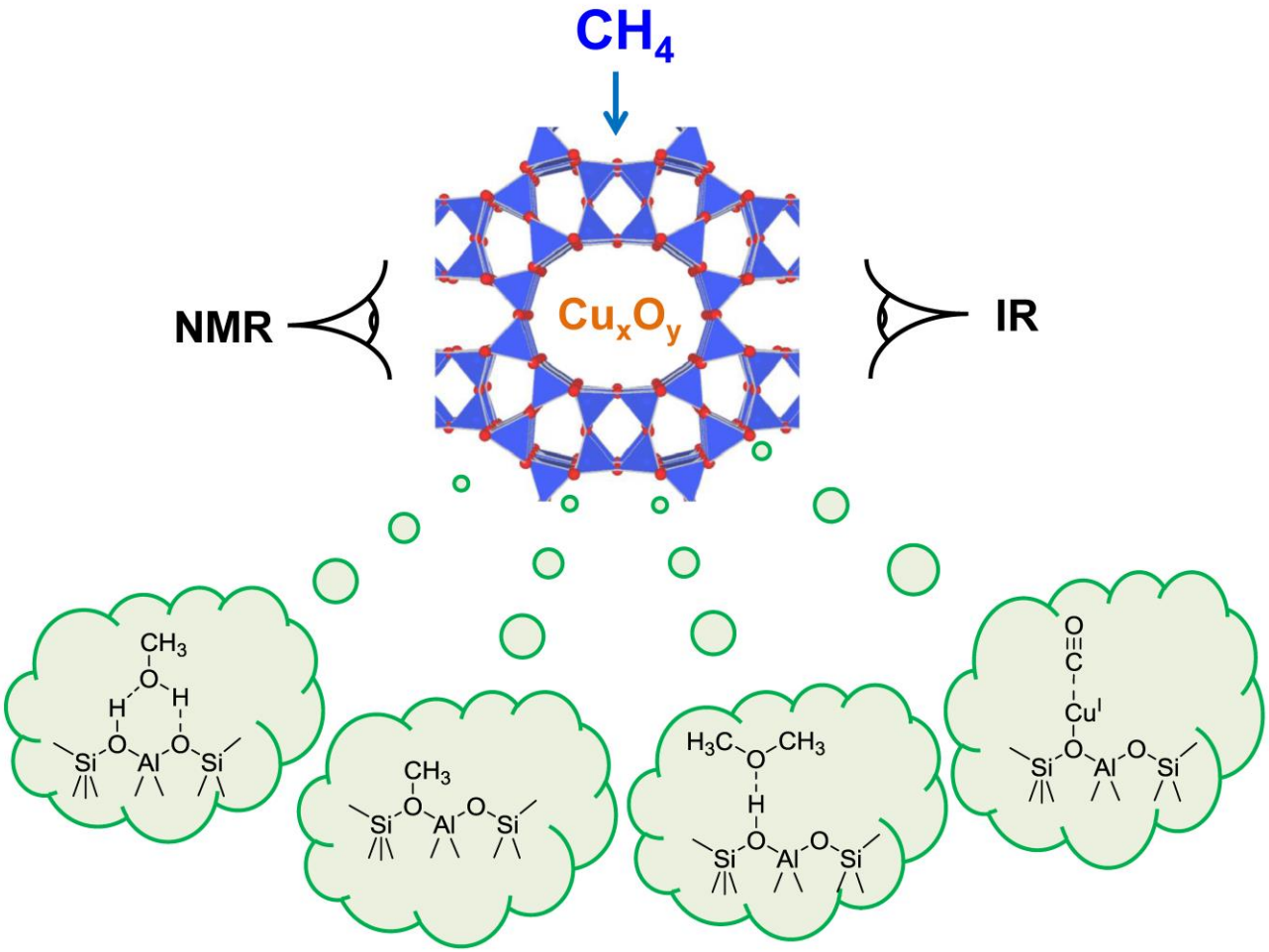

Accepted Manuscript

This article is protected by copyright. All rights reserved.